The Astrophysical Journal, 889:176 (13pp), 2020 February 1 https://doi.org/10.3847/1538-4357/ab5303

WISE 2150-7520AB: A Very Low-mass, Wide Comoving Brown Dwarf System Discovered through the Citizen Science Project Backyard Worlds: Planet 9*

Jacqueline K. Faherty[1], Sam Goodman[2], Dan Caselden[2], Guillaume Colin[2], Marc J. Kuchner[3], Aaron M. Meisner[4,11], Jonathan Gagné[5], Adam C. Schneider[6], Eileen C. Gonzales[1,7,8], Daniella C. Bardalez Gagliuffi[1], Sarah E. Logsdon[3,12], Katelyn Allers[9], and Adam J. Burgasser[10]
The Backyard Worlds: Planet 9 Collaboration[2]
[1] Department of Astrophysics, American Museum of Natural History, Central Park West at 79th Street, NY 10024, USA; jfaherty@amnh.org
[2] Backyard Worlds: Planet 9
[3] NASA Goddard Space Flight Center, Exoplanets and Stellar Astrophysics Laboratory, Code 667, Greenbelt, MD 20771, USA
[4] National Optical Astronomy Observatory, 950 N. Cherry Ave., Tucson, AZ 85719, USA
[5] Institute for Research on Exoplanets, Université de Montréal, 2900 Boulevard Édouard-Montpetit Montréal, QC Canada H3T 1J4, Canada
[6] School of Earth and Space Exploration, Arizona State University, Tempe, AZ 85282, USA
[7] The Graduate Center, City University of New York, New York, NY 10016, USA
[8] Department of Physics and Astronomy, Hunter College, City University of New York, New York, NY 10065, USA
[9] Physics and Astronomy Department, Bucknell University, 701 Moore Ave, Lewisburg, PA 17837 Norman, OK 73019, USA
[10] Department of Physics, Center for Astrophysics and Space Sciences, Mail Code 0424, 9500 Gilman Drive, La Jolla, CA 92093-0424, USA; aburgasser@ucsd.edu
Received 2019 August 1; revised 2019 October 28; accepted 2019 October 29; published 2020 February 4

Abstract

We report the discovery of WISE 2150-7520AB (W2150AB): a widely separated (∼341 au) very low-mass L1 + T8 co-moving system. The system consists of the previously known L1 primary 2MASS J21501592-7520367 and a newly discovered T8 secondary found at position 21:50:18.99–75:20:54.6 (MJD = 57947) using *Wide-field Infrared Survey Explorer* data via the Backyard Worlds: Planet 9 citizen science project. We present *Spitzer ch*1 and *ch*2 photometry (*ch*1–*ch*2 = 1.41 ± 0.04 mag) of the secondary and Folded-port InfraRed Echellette prism spectra of both components. The sources show no peculiar spectral or photometric signatures, indicating that each component is likely field age. Using all observed data and the *Gaia* DR2 parallax of 41.3593 ± 0.2799 mas for W2150A we deduce fundamental parameters of $\log(L_{\rm bol}/L_\odot) = -3.69 \pm 0.01$, $T_{\rm eff} = 2118 \pm 62$ K, and an estimated mass = 72 ± 12 $M_{\rm Jup}$ for the L1 and $\log(L_{\rm bol}/L_\odot) = -5.64 \pm 0.02$, $T_{\rm eff} = 719 \pm 61$ K, and an estimated mass = 34 ± 22 $M_{\rm Jup}$ for the T8. At a physical separation of ∼341 au this system has $E_{\rm bin} = 10^{41}$ erg, making it the lowest binding energy system of any pair with $M_{\rm tot} < 0.1\,M_{\rm Sun}$ not associated with a young cluster. It is equivalent in estimated mass ratio, $E_{\rm bin}$, and physical separation to the ∼2 Myr M7.25 + M8.25 binary brown dwarf 2MASS J11011926-7732383AB (2M1101AB) found in the Chameleon star-forming region. W2150AB is the widest companion system yet observed in the field where the primary is an L dwarf or later.

Unified Astronomy Thesaurus concepts: Brown dwarfs (185); L dwarfs (894); Substellar companion stars (1648); Astrometry (80); Star formation (1569); T dwarfs (1679); Late-type dwarf stars (906); Stellar kinematics (1608)

Supporting material: machine-readable tables

1. Introduction

Brown dwarfs are a unique population of astronomical objects and a critical bridge between stars and planets. On the high-mass end, brown dwarfs overlap in observable properties with the coolest stars like TRAPPIST-1 which hosts seven terrestrial worlds (Gillon et al. 2017). On the low-mass end, brown dwarfs overlap with the observable properties of directly imaged exoplanets like 51 Eri b (Macintosh et al. 2015) and Beta Pictoris b (Lagrange et al. 2010). On the coolest end, brown dwarfs like J085510.83-071442.5—a ∼250 K object at just 2 pc from the Sun (Luhman 2014)—are directly comparable to Jupiter (Skemer et al. 2016; Morley et al. 2018).

Studying brown dwarfs provides insight into stellar and planetary atmospheres and activity. One of the most important and outstanding questions in substellar mass science is how these objects form and evolve. Co-moving companions are a key sub-population for investigating questions of formation.

Early searches for low-mass companions resulted in two distinct categories of objects: those that were either (1) well-resolved companions discovered through common proper motion or closely separated and with statistically consistent distances (e.g., Kirkpatrick et al. 2001; Wilson et al. 2001; Faherty et al. 2010) or those that were (2) closely bound and discovered through high-resolution imaging (e.g., Martin et al. 1999; Koerner et al. 1999; Burgasser et al. 2003). For several years the only objects that fell in category (1) were brown dwarfs orbiting higher-mass stars (mass ratios $\ll 1$) and those that fell in category (2) were near-equal-mass binaries (mass ratio ∼ 1) with very low total masses ($\sim 0.1\,M_\odot$) and binding energies.

Work done on young clusters such as Taurus, Rho Ophiucus, and Chameleon resulted in the discovery of widely separated objects (>100 au) with mass ratios near 1 and small total masses that were hybrids between the two previously distinct classes (e.g., Luhman 2004; Close et al. 2007). Searches in the field also turned up a handful of objects that were widely

* This paper includes data gathered with the 6.5 m Magellan Telescopes located at Las Campanas Observatory, Chile.
[11] Hubble Fellow.
[12] NASA Postdoctoral Program Fellow.

separated with relatively low total masses, though nothing that rivaled the low binding energies found among young cluster companions (e.g., Artigau et al. 2007; Radigan et al. 2009).

Brown dwarf spectral classification categories include L, T, and Y dwarfs (e.g., Kirkpatrick et al. 1999; Burgasser et al. 2006; Cushing et al. 2011; M dwarfs are almost exclusively stellar unless young). In the absence of dynamical mass measurements, an age is required to determine whether an object of a given spectral class has a mass that is above or below the hydrogen burning limit. However the L, T, and Y classes are all definitively in the low-temperature regime for compact sources (e.g., Vrba et al. 2004; Dupuy & Kraus 2013; Tinney et al. 2014; Filippazzo et al. 2015). Consequently, the bulk of ultracool dwarf companions (e.g., L+L, L+T, T+T, T+Y) have been found in category (2): closely bound and unresolved in all but high-resolution imaging. Until this work there were only two easily resolved visual L+T binaries: SDSS J1416+13AB (Burningham et al. 2010) which is an L7+T7.5 binary with an angular separation of $9\farcs81$ or a physical separation of 89.3 ± 1.5 au at the system's distance of 9.1 ± 0.15 pc (Dupuy & Liu 2012) and Luhman 16AB (Luhman 2013) which is an L7.5+T0.5 binary with an angular separation of $1\farcs5$ or a physical separation of ~3 au at the system's distance of 2.02 ± 0.019.

Brown dwarf formation theories are specific in their predictions of binary parameters. Model scenarios that involve ejection (e.g., Reipurth & Clarke 2001; Bate et al. 2002; Bate 2011), turbulent fragmentation (e.g., Padoan & Nordlund 2004), and/or disk fragmentation (e.g., Goodwin & Whitworth 2007; Li et al. 2015) to produce brown dwarfs predict statistical properties which can be compared to observational studies as evidence for or against formation pathways. In general, theoretical models do not produce very low-mass binaries ($M_{\rm tot} < 0.1\,M_{\rm Sun}$) with separations >10 au (e.g., Bate et al. 2002) that can survive to field age. This prediction is roughly consistent with the very low-mass wide binary population of near-equal-mass companions. The exceptions are those found in clusters and the handful of slightly higher-mass wide objects. This dearth of observed widely separated companions was attributed to their being thought not to exist or not to survive to field age.

In this paper we report the discovery of a wide, very low-mass co-moving system consisting of an L1 and T8 discovered through the citizen science project Backyard Worlds: Planet 9. Section 2 reviews how the discovery was made. Section 3 describes new data acquired on the primary and secondary sources in the system. Section 4 has observational details on each component. Section 5 discusses the *Gaia* parallax, kinematics of each component, and probability of chance alignment. Section 6 has the color–magnitude diagram analysis for the system while Section 7 reviews the age. Section 8 details the fundamental parameters for each component and Section 9 has the binding energy analysis. Conclusions are summarized in Section 10.

2. Discovery

The Backyard Worlds: Planet 9 citizen science project (Backyard Worlds for short) has been operational since 2017 February. The scientific goal of the project is to complete the census of the solar neighborhood (including the solar system, e.g., Planet 9) with objects that are detectable primarily at mid-infrared wavelengths and that were missed by previous searches (see Kuchner et al. 2017 and Debes et al. 2019). Backyard Worlds utilizes multiple epochs of NASA's *Wide-field Infrared Survey Explorer* (*WISE*) mission at both *W1* (~3.5 μm) and *W2* (~4.5 μm) wavelengths. Project participants are asked to blink between four unWISE images (see Meisner et al. 2017a) where the time-span between the first and last image is ~4.5 yr. Given this time baseline, objects of significant motion (e.g., >200 mas yr^{-1}) are relatively easy to visually identify (see for example Kuchner et al. 2017).

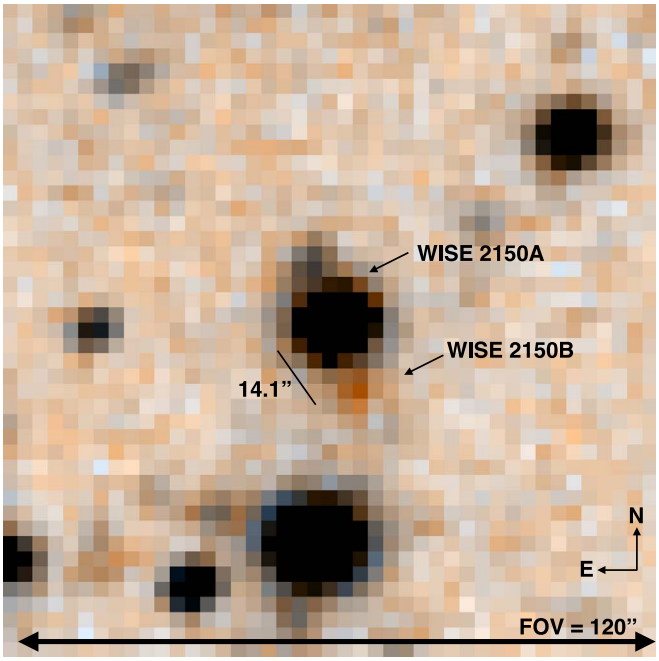

Figure 1. Finder chart for the W2150AB system taken from the WISEVIEW website (Caselden et al. 2018). To see the animated motion between available *WISE* epochs visit the URL http://byw.tools/wiseview and use coordinates R. A., decl. = 327.576919, −75.34805934. The color choice combines *WISE W1* and *W2* images where "orange" sources are strong *W2* and weak *W1* detections.

The BackyardWorlds.org website hosted by Zooniverse provides two avenues for reporting a proper motion candidate of scientific interest to the Backyard Worlds research team. The first is by using the web portal to blink *WISE* epoch images and "click" on an object that appears to move over the ~4.5 yr baseline. Once identified, these objects go into a large repository that the research team can access through Zooniverse. The second avenue for reporting a candidate is to alert the science team by submitting the coordinates and details of the source on a Google form labeled "Think You've Got One."

Three citizen science users (co-authors S. Goodman, D. Caselden, and G. Colin) brought to our attention a *WISE W2*-only detected source with significant motion. They used the Google form and emphasized the objects importance by emailing the Backyard Worlds distribution list as well as key researchers on our team. In addition, these users easily noted a bright source $14\farcs1$ away that appeared to be co-moving. Upon further investigation the users realized this was the known L1 dwarf SIPS J2150-7520 (or source 2MASS J21501592-7520367; Deacon et al. 2005). On 2018 June 29, the motion of W2150B was vetted by the research team and added to our high-priority follow-up target list. Figure 1 shows a screenshot from the WISEVIEW website (Caselden et al. 2018) which was used to identify and confirm the system.

3. Data

We obtained both near-infrared spectra and mid-infrared photometry for the system WISE 2150-7520AB (W2150AB).

3.1. Magellan FIRE Spectroscopy

We used the 6.5 m Baade Magellan telescope and the Folded-port InfraRed Echellette (FIRE; Simcoe et al. 2013) spectrograph to obtain near-infrared spectra of both the primary and the secondary in this system. Observations were made on 2018 December 1 under clear conditions. For all observations, we used the prism mode and the 0.″6 slit (resolution $\lambda/\Delta\lambda \sim 100$) covering the full 0.8–2.5 μm band. We observed the A component using a standard ABBA nod pattern with an exposure time of 90 s per nod. For the B component we obtained an ABBAAB nod pattern with an exposure time of 120 s per nod. Immediately after the B component, we observed the A star HD 200523 for telluric correction and obtained a Ne–Ar lamp spectrum for wavelength calibration. At the start of the night we used quartz lamps as domeflats in order to calibrate pixel-to-pixel response. Data were reduced using the FIREHOSE package which is based on the MASE and SpeXtool reduction packages (Vacca et al. 2003; Cushing et al. 2004; Bochanski et al. 2009).

3.2. Spitzer *Photometry*

The field surrounding W2150B was observed by the *Spitzer Space telescope* on 2018 December 7. Data were obtained in both *ch*1 and *ch*2 bands. Peak-up was disabled and each filter was observed using a 16-position spiral dither pattern with 30 s per frame. The readout was done in full array mode. Data were downloaded and aperture photometry was performed on the *Spitzer* Heritage reduced mosaic images.

4. Details on the Components

4.1. Primary

W2150A was originally reported as a proper motion source with red optical and near-infrared colors reminiscent of a late-type M/early L dwarf in Deacon et al. 2005 (originally called SIPS J2150-7520 and identified in 2MASS as 2MASS J21501592-7520367). It was followed up with optical spectroscopy by Reid et al. (2008) and published as an L1 ± 1. Subsequently, the proper motion was updated for this object in Casewell et al. (2008) and Faherty et al. (2009). Faherty et al. (2010) specifically looked for co-moving companions to known M and L dwarfs but nothing of note was recovered around W2150A in either the *Hipparcos* or LSPM catalogs.

In Figure 2 we plot the optical spectrum from Reid et al. (2008) and the near-infrared spectrum obtained with FIRE highlighting prominent spectral features. Overplotted on each is the L1 near-infrared standard 2MASSW J2130446-084520. The sources are normalized by the maximum flux over the wavelength covered (*J*, *H*, and *K*). In the optical, Hα and Li I absorption are indicators of activity as well as mass (hence age). The optical spectrum of W2150A shows no detectable Li I or Hα absorption or emission although the noise is significant. There is also no Rb I or appreciable Cs I detected although this may be due to the low resolution of the data. The near-infrared spectrum receives a field gravity designation

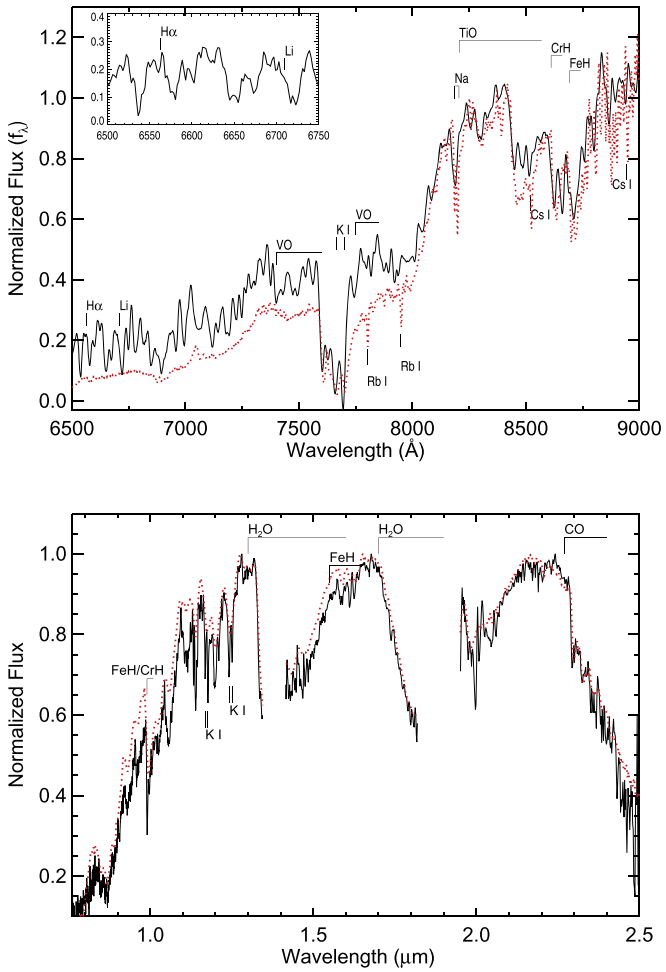

Figure 2. Top: optical spectrum of W2150A (black solid line) from Reid et al. (2008) compared to the L1 standard 2MASSW J2130446-084520 (red dashed; also from Reid et al. 2008). Prominent spectral absorption features are highlighted. The region surrounding the Hα and Li I features is contained in the inset; we find no detection of either. Bottom: infrared spectrum of W2150A (black solid line) obtained using the FIRE spectrograph in prism mode (this work), normalized to the peak in each band (*JHK*). We compare this spectrum to that of the L1 standard 2MASSW J2130446-084520 (red dashed curve) from Kirkpatrick et al. (2010). Prominent near-infrared features are labeled.

using the Allers & Liu (2013) spectral indices and we see no visible signatures of low surface gravity.

Figure 3 shows the colors and absolute magnitudes from 2*M*ASS through *WISE* for W2150A compared to median values of field objects as listed in Faherty et al. (2016). W2150A shows no deviation and fits within 1σ of seemingly normal equivalent type objects. All positional, photometric, and kinematic data are listed in Table 1.

4.2. Secondary

At the time of its initial discovery, W2150B had not been detected in any previously published *WISE* catalog (for example it was in neither AllWISE nor the *WISE* All-Sky catalog) nor any publicly accessible catalog (e.g., it was also not in 2MASS). After citizen scientists reported the source at position 21:50:18.99–75:20:54.6 (MJD = 57947), the research team checked the unWISE Catalog for a detection (Lang 2014; Meisner et al. 2017b; Schlafly et al. 2019) and found that the source was faint ($W2 = 16.01 \pm 0.06$) and red in the *WISE* bands ($(W1–W2) = 2.42 \pm 0.15$). This red color, combined

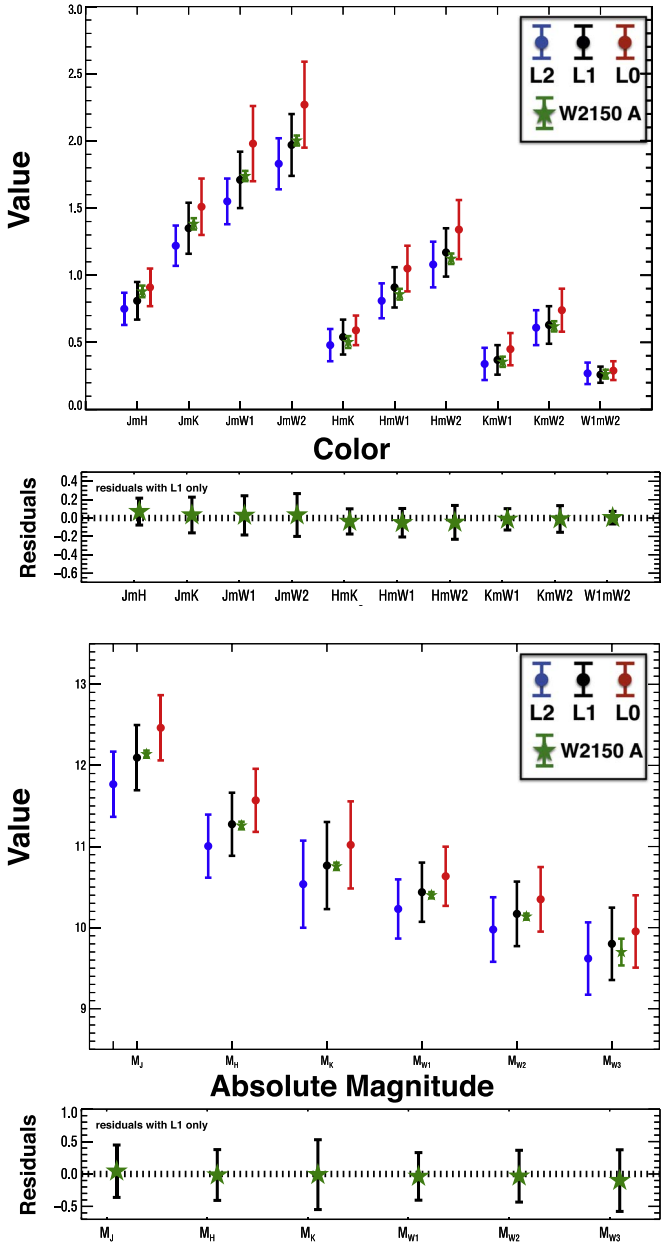

Figure 3. Top: average colors and their spread for 2MASS *JHK* through *WISE* *W1W2* bandpasses for field L0 (red), L1 (black), and L2 (blue) dwarfs as listed in Faherty et al. (2016). We show the values calculated for W2150A with uncertainties as a five-point star colored in green. Bottom: average absolute magnitudes and their spread as above. The values for W2150A are calculated using 2*M*ASS and *WISE* photometry as well as the *Gaia* DR2 parallax.

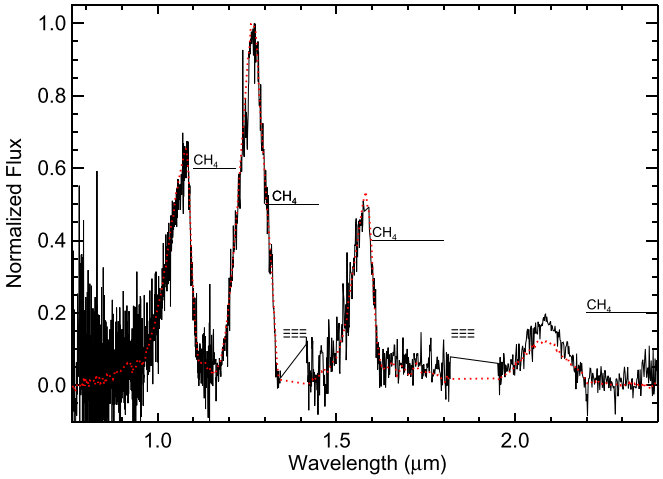

Figure 4. FIRE prism spectrum of W2150B (black curve) compared to a spectrum of the T8 standard 2MASSI J0415195-093506 (red curve) from Burgasser et al. (2004). The spectra have been normalized by the maximum flux over all the data.

with the source's significant motion, were a tell-tale sign that the object was a close and cold brown dwarf.

The unWISE catalog provides valuable information about W2150B, but the photometry in this catalog was derived from the full 2010–2017 unWISE stack, with no attempt made to account for the considerable ∼7″ of source motion during that time span. We therefore performed additional custom *WISE* astrometry and photometry using coadds binned into yearly time intervals (Meisner et al. 2018). We bin into yearly intervals because W2150B is so faint that coaddition of two six-month *WISE* sky passes is necessary to form one measurement epoch. The field surrounding W2150B was observed by *WISE* in two separate sky passes during 2010 (mean MJD = 55402), 2015 (mean MJD = 57198), 2016 (mean MJD = 57580), and 2017 (mean MJD = 57947). The field should have also been observed by *WISE* in 2014 April, but due to a command timing anomaly, the location suffered a missed sky pass. We therefore omit calendar year 2014 *WISE* data from our analysis. Combining measurements from the remaining four coadds yields $W2 = 15.81 \pm 0.05$ mag. This value agrees well with the *W*2 estimate reported in the unWISE catalog, with the latter being slightly faint due to its smeared point-spread function. The source is marginally detected in *W*1 yearly coadds and therefore we did not attempt to redo photometry in this band. Instead we adopt $W1 = 18.18 \pm 0.15$, which is the unWISE catalog mag with a correction to account for the smearing due to the high proper motion of the source. W2150B was observed in *Spitzer* GO program 14076 and both *ch*1 and *ch*2 photometry were acquired to verify the cold nature of the source. We measured a (*ch*1–*ch*2) color for the object of 1.41 ± 0.04 mag. According to the Kirkpatrick et al. (2019) color spectral type relations, the (*ch*1–*ch*2) and (*W1*–*W2*) colors correspond to a spectral type of T7 ± 1.

The FIRE prism spectrum for W2150B is shown in Figure 4 and appears most like a field T8. The source matches the T8 infrared standard well, with the exception of enhanced flux seen in the *K* band.

Using the *Gaia* parallax of the primary, we computed absolute magnitudes in *WISE* *W1W2* and *Spitzer* *ch*1*ch*2 bands. Figure 5 shows a suite of absolute magnitude versus spectral type diagrams featuring the *WISE* and *Spitzer* bandpasses discussed in this work. W2150B falls within the spread of normal field T8 objects discussed in Kirkpatrick et al. (2019).

Figure 6 shows the color–magnitude diagrams for brown dwarfs in *WISE* and *Spitzer* bands. Assuming the *Gaia* DR2 parallax for W2150B (see Section 6), its absolute magnitudes in each band are on the faint side for its color. It remains unclear if such a position on color–magnitude diagrams might indicate slightly deviant cloud, metallicity or gravity properties (e.g., Tinney et al. 2014; Leggett et al. 2017).

In summary, W2150B appears to be a spectrally normal field T8 dwarf. It is well matched to the absolute magnitudes of known similar type objects yet slightly faint for its color in all bands. All positional, photometric, and kinematic data are listed in Table 1.

Table 1
Measured Parameters

Parameter (1)	W2150A (2)	W2150B (3)	System (4)	Units (5)	Reference (6)
ASTROMETRY					
α	327.58083685735[a] (±0.2 mas)	327.579158[b] (±0.6 mas)	...	deg	1, 2
δ	−75.34482002123[a] (±0.3 mas)	−75.348499[b] (±0.6 mas)	...	deg	1, 2
ℓ[a]	315.9126	...	...	deg	1
b[a]	−36.8406	...	...	deg	1
ϖ	41.3593 ± 0.2799	...	...	mas	1
μ_α	888.627 ± 0.502	876 ± 45	...	mas yr^{-1}	1, 2
μ_δ	−298.234 ± 0.518	−278 ± 45	...	mas yr^{-1}	1, 2
PHOTOMETRY					
G_{BP}	21.4462 ± 0.2021	...	...	mag	1
G	18.9110 ± 0.0038	...	...	mag	1
G_{RP}	17.3031 ± 0.0118	...	...	mag	1
I	17.53 ± 0.17	...	...	mag	5
J	14.056 ± 0.029	(19.03 ± 0.23)[c]	...	mag	3
H	13.176 ± 0.032	(19.24 ± 0.22)[c]	...	mag	3
K_s	12.673 ± 0.030	...	...	mag	3
$W1$[d]	12.317 ± 0.024	18.18 ± 0.15	...	mag	4, 2
$W2$[d]	12.053 ± 0.023	15.81 ± 0.05	...	mag	4, 2
$W3$[d]	11.616 ± 0.150	...	...	mag	4
$W4$[d]	<9.328	...	...	mag	4
$ch1$	...	17.01 ± 0.03	...	mag	2
$ch2$	...	15.60 ± 0.02	...	mag	2
SPECTROSCOPY					
Spectral type (OpT)	L1 ± 1	...	...	...	2
Spectral type (IR)	L1 ± 1	T8 ± 1	...	...	2
FUNDAMENTALS					
Age	0.5–10	0.5–10	0.5–10	Gyr	2
$\log(L_{\rm bol}/L_\odot)$	−3.69 ± 0.01	−5.64 ± 0.02	...	...	2
$T_{\rm eff}$	2118 ± 62	719 ± 61	...	K	2
Radius	1.03 ± 0.06	0.95 ± 0.16	...	$R_{\rm Jup}$	2
Mass	72 ± 12	34 ± 22	...	$M_{\rm Jup}$	2
log$g$	5.2 ± 0.2	4.9 ± 0.5	...	...	2
KINEMATICS					
Distance[e]	24.18 ± 0.16	27 ± 4[f]	24.18 ± 0.16	pc	2
$v_{\rm tan}$[g]	107.43 ± 0.06	117 ± 6	107.43 ± 0.06	km s^{-1}	2
ABS MAGS					
M_G	16.99 ± 0.02	...	...	mag	2
M_I	15.61 ± 0.17	...	...	mag	2
M_J	12.14 ± 0.03	...	...	mag	2
M_H	11.26 ± 0.03	...	...	mag	2
M_K	10.76 ± 0.03	...	...	mag	2
M_{W1}	10.43 ± 0.03	16.26 ± 0.15	...	mag	2
M_{W2}	10.16 ± 0.03	13.89 ± 0.05	...	mag	2
M_{W3}	9.55 ± 0.16	...	...	mag	2
M_{ch1}	...	15.09 ± 0.03	...	mag	2
M_{ch2}	...	13.68 ± 0.03	...	mag	2
SYSTEM					
Separation	...	...	14.1	$''$	2
Separation	...	...	341	au	2
Binding energy	...	...	1.004	10^{41} erg	2

Notes. The object does not have entries in GSC 2.2, USNO-B1.0, and does not appear on any of the photographic sky surveys scanned by SuperCOSMOS.
[a] epoch J2015.5, ICRS
[b] Calculated using *WISE* image at MJD = 57947.
[c] The 2MASS J and H magnitudes are estimates from the expected J–$W2$ and H–$W2$ colors of a T8. We used the sample of brown dwarfs in Kirkpatrick et al. (2011) to estimate an offset of 3.21 ± 0.23 mag for 2MASS J and 3.43 ± 0.23 mag for 2MASS H from the *WISE* $W2$ magnitude.
[d] For the L1 primary, we chose the original *WISE* catalog values in the analysis over the AllWISE values so we could compare to the photometry in Faherty et al. (2016), For the T8 secondary $W2$ comes from the yearly $W2$ coadd analysis of Section 4.2, and $W1$ comes from the unWISE Catalog (Schlafly et al. 2019) with a correction applied for source motion.
[e] Calculated using $D = 1/\pi$, which is a good approximation for a parallax known to $\pi/\sigma_\pi = 133$ accuracy.
[f] Calculated using the M_{W2} from the SpT relation in Kirkpatrick et al. (2019).
[g] Calculated using Lindegren et al. (2018) astrometry.
References. (1) Lindegren et al. (2018), (2) this paper, (3) Cutri et al. (2003), (4) Wright et al. (2010), (5) DENIS Consortium (2005).

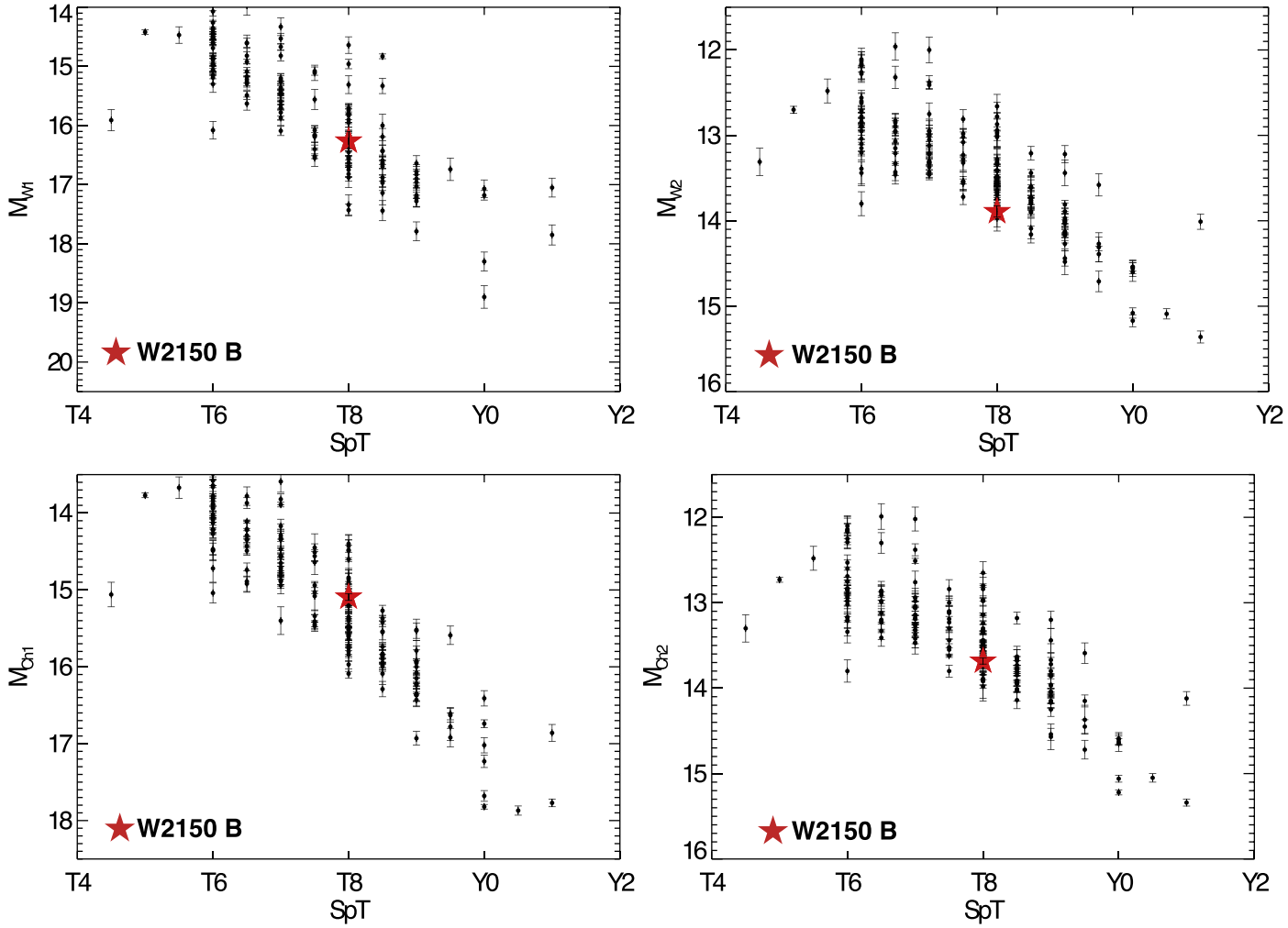

Figure 5. Absolute magnitude vs. spectral type diagram for W2150B in the *WISE* and *Spitzer* bandpasses. The mid- to late-type T comparative sample comes from Kirkpatrick et al. (2019) with a few earlier type sources from Dupuy & Liu (2012).

5. *Gaia* with Probability of Chance Alignment

Using the WISEVIEW motion visualization tool (Caselden et al. 2018),[13] the motions of both the primary and secondary are obvious (see Figure 1 for a screenshot). After cross-matching with the *Gaia* DR2 catalog release (Gaia Collaboration et al. 2016; Lindegren et al. 2018) citizen scientist and co-author S. Goodman reported that the primary was also source *Gaia* DR2 6358287868675805824 and had a well measured parallax and proper motion. The *Gaia* parameters for 2M2150A—which we assume as the astrometry for the system—are listed in Table 1.

While the WISEVIEW animation clearly shows the two sources are moving at a similar rate, we computed the proper motion for W2150B by examining the yearly *WISE* coadds of Section 4.2 in combination with the *Spitzer* position. As we mentioned in Section 4.2, there are four yearly *WISE* coadds for W2150B with mean MJDs of 55402, 57198, 57580, and 57947. Including the *Spitzer* image taken at MJD = 58459 provides an 8.37 yr baseline between the first and last position measurements. We calculated $(\mu_{\rm ra}\cos(\rm decl.), \mu_{\rm decl.}) = (876 \pm 45, -278 \pm 45)$ mas yr^{-1} and found that our calculated proper motions in both R.A. and decl. for W2150B are within 1σ of the *Gaia* DR2 values for W2150A. All kinematic information for W2150B is listed in Table 1.

To quantify the probability that the system might be a chance alignment, we examined the 100 pc *Gaia* DR2 catalog and found all the objects with proper motion component and parallax values that fell within 1σ of W2150B. Out of the 700,055 stars there were four matches including W2150A. W2150A is $<15''$ away while the three other matches were scattered across the sky (hundreds of degrees away). We ran a Monte Carlo simulation with 90,000 iterations of randomly moving stars to determine that there was a 0.00007% likelihood that W2150A is a chance coincidence with W2150B (at an angular separation of $<15''$).

Furthermore, the *Gaia* DR2 parallax for W2150A matches within 1σ with the estimated spectrophotometric distance for W2150B that comes from the spectral type relations in Kirkpatrick et al. (2019) (see Section 4.2 and Table 1).

6. Color–Magnitude Diagrams for the System

For all analysis that follows, we assume that W2150AB is a physically associated, co-evolving system; therefore we use

[13] D. Caselden is also one of the citizen scientist co-discoverers of this binary.

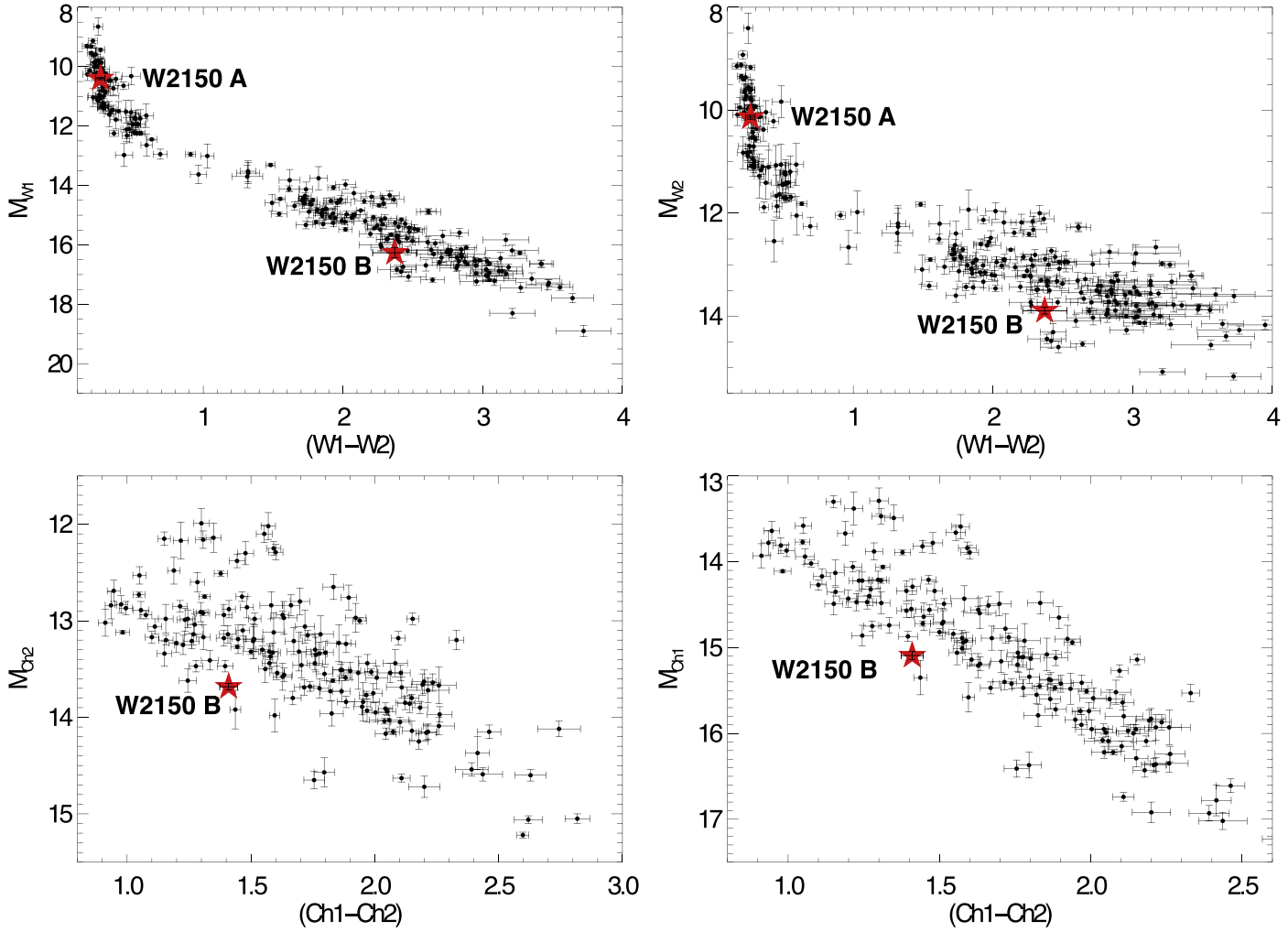

Figure 6. Color–magnitude diagrams for L through late-type T/Y dwarfs with W2150AB highlighted. The top panels show *WISE* color–magnitude diagrams and both the primary and secondary. The bottom panels show *Spitzer* color–magnitude diagrams, including only the secondary. The mid- to late-type T dwarfs in the comparative sample come from Kirkpatrick et al. (2019) and the earlier type objects come from Dupuy & Liu (2012) and Faherty et al. (2012).

the *Gaia* parallax of the primary for the secondary as well. We examined both sources on color–magnitude diagrams to investigate commonality or differences in their positions relative to the field sequence. The top panels of Figure 6 show the *WISE* color–magnitude diagrams for field L through late-type T dwarfs with both W2150A and W2150B highlighted. While W2150A sits well within the locus of field sources, W2150B is faint and/or blue compared to equivalent sources. Given that we also had *Spitzer* photometry for the secondary and there is an array of trigonometric parallax and photometric data on late-type sources from the Kirkpatrick et al. (2019) program, we also show the *Spitzer* color–magnitude diagrams in the bottom panels of Figure 6. Similar to the *WISE* diagrams, W2150 B appears slightly faint and/or blue for its given color compared to the field sequence. This position suggests that the source has lower metallicity and hence is older than the field population (e.g., Leggett et al. 2010); however, nothing conclusive can be drawn at this time. The primary shows no indications of high surface gravity and none of the classic low-metallicity/subdwarf spectral indicators (e.g., Burgasser et al. 2004; Cushing et al. 2009; Kirkpatrick et al. 2014, 2016; Gonzales et al. 2018).

7. Discussion on the Age of the System

Identifying the age of a brown dwarf is an extremely difficult task. Solar-type stars have a suite of diagnostics to estimate the age range of an object such as gyrochronology, astroseismology, chromospheric activity, and Li I depletion (see, e.g., Pavlenko & Magazzu 1996; Barnes 2007; Mamajek & Hillenbrand 2008). However, brown dwarfs have relatively few diagnostic tools largely due to their low temperatures and lack of stable core nuclear burning. There are a handful of emerging diagnostics but they are not precisely calibrated. For instance, spectral features like alkali lines, metal oxide and hydride bands, and overall *H* band shape can strongly indicate whether an object is low/high surface gravity, hence young/old (see, e.g., Cruz et al. 2009; Allers & Liu 2013). Near-infrared colors combined with spectral type and kinematics can also indicate sub-populations of brown dwarfs that are redder/slower/younger or bluer/faster/older. While there are now several L and T dwarfs known in nearby moving groups (e.g., Liu et al. 2013, 2016; Artigau et al. 2015; Faherty et al. 2016, 2013; Gagné et al. 2017, 2018; Riedel et al. 2019) as well as substellar mass subdwarfs (e.g., Burgasser et al. 2003; Kirkpatrick et al. 2014), age diagnostics show significant scatter and are not established for field age objects.

Co-moving systems are excellent sources of calibration for age diagnostics. For this purpose, one would like to find a brown dwarf co-moving with a higher-mass companion (solar-type star for instance), take an age diagnostic for the primary and apply it to the secondary to calibrate its observable features (see, e.g., Faherty et al. 2010, 2011; Kirkpatrick et al. 2010; Mužić et al. 2012; Burningham et al. 2013; Deacon et al. 2014). The case of W2150AB is intriguing because it is two well resolved ultracool dwarf objects orbiting each other. By examining their spectral features and positions on color–magnitude and spectral photometric diagrams in tandem we can investigate whether there are any common age-diagnostic trends in their values. However, as noted above, neither object shows peculiar spectral features. While W2150B appears slightly faint for its given *WISE* or *Spitzer* color, neither it nor W2150A is in a particularly extreme part of any diagram.

The total tangential velocity of the system is $>100\,\mathrm{km\,s^{-1}}$ (as shown in Table 1), which is notable especially given the position of W2150B on Figure 6. Faherty et al. (2009) found that objects with vtan $>100\,\mathrm{km\,s^{-1}}$ also tended to be those that were particularly blue for their spectral types and yielded older kinematic ages. Since neither source is particularly deviant in its colors, we conclude that both components are of field age, possibly tending toward the older range of field sources. While there are differing results on what "field age" might mean for L and T dwarfs, recent results from Burgasser et al. (2015) show that L dwarfs within ∼20 pc have kinematic mean ages of 6.5 ± 0.4 Gyr. However we can only conclude that the L dwarf receives a field gravity using spectral indices and neither the L nor the T dwarf shows features of a halo subdwarf. Consequently we adopt a broad age range for this system; it appears to be older than 500 Myr and younger than ∼10 Gyr, a conservative cap on the age of field sources.

8. Fundamental Parameters

Following the prescription of Filippazzo et al. (2015), we use the *Gaia* DR2 parallax of W2150A combined with all available photometric and spectroscopic information to produce distance-calibrated spectral energy distributions (SEDs) for the two sources. By integrating over these SEDs, we directly calculate their bolometric luminosities. Using the evolutionary models of Saumon & Marley (2008) paired with the age range cited above, we obtain a radius range for each source and semi-empirically obtain estimates for the $T_{\rm eff}$, mass, and $\log g$. For W2150A we used the *Gaia* G, 2MASS JHK, and *WISE W1W2W3* photometry along with the optical and near-infrared spectra to extract information. For W2150B we only have the *WISE W1W2* bands and *Spitzer ch*1ch2 bands along with the FIRE prism spectrum. The Filippazzo et al. (2015) method requires at least a near-infrared estimate of photometry to scale the spectrum, therefore we estimated the 2MASS *J* and *H* bands using offsets computed from *WISE*- and 2MASS-detected T8 objects in Kirkpatrick et al. (2011) (see Table 1 for details).

We find that W2150A has $\log(L_{\rm bol}/L_\odot) = -3.69 \pm 0.01$, $T_{\rm eff} = 2118 \pm 62$ K, $\log g = 5.2 \pm 0{,}2$, radius $= 1.03 \pm 0.06 R_{\rm Jup}$ and an estimated mass $= 72 \pm 12\,M_{\rm Jup}$ while the T8 has $\log(L_{\rm bol}/L_\odot) = -5.64 \pm 0.02$, $T_{\rm eff} = 719 \pm 61$ K, $\log g = 4.9 \pm 0,\ 5$, radius $= 0.95 \pm 0.16\,R_{\rm Jup}$ and an estimated mass $= 34 \pm 22\ M_{\rm Jup}$. All of these fundamental parameter values are listed in Table 1; they appear consistent with field sources discussed in Filippazzo et al. (2015).

9. Binding Energy

Early studies of very low-mass binaries concluded that there was a minimum binding energy (E_b) required for systems to form and remain stable. Works such as Close et al. (2003) and Burgasser et al. (2003) determined E_b for field ultracool dwarf to ultracool dwarf pairs of $\sim 2 \times 10^{42}$ erg. However, as Faherty et al. (2010) have discussed, searches in recent years have revealed numerous field-age and young wide companions falling well below the previously considered minimum binding energy (e.g., Luhman 2004; Burgasser 2007; Artigau et al. 2009; Radigan et al. 2009). We attempted to compile an up-to-date sample of very low-mass binaries/companions, drawing from both large survey papers such as Deacon et al. (2014), spectral binary papers such as Bardalez Gagliuffi et al. (2014), and individual young companion papers such as Artigau et al. (2015), and Naud et al. (2014). Figures 7 and 8 display a compilation of binary (or co-moving) systems from various catalogs. We list the objects displayed in Figures 7 and 8 with $M_{\rm tot} < 0.2\,M_{\rm Sun}$ organized by increasing binding energy in Table 2. Additionally we searched the *Gaia* DR2 catalog to see if either the primary or secondary component had astrometry and/or photometry reported and we list the results in Table 3.

We separate the different sub-populations of companion systems thought to be younger than 1 Gyr and those older on Figure 7. The top panel of Figure 7 shows separation versus total mass of the system and allows us to examine if there is a distinguishable distance which would delineate where systems become unstable and disperse. The bottom panel of Figure 8 shows the total mass of the system versus binding energy, allowing us to investigate if there is a minimum value required for formation or survival within the Galaxy. We find that W2150AB occupies a unique space on the upper and lower panels of Figure 7. It is surrounded by only young sources with comparable low binding energy objects in the field with higher total masses. It is the only L plus T dwarf co-moving system with a separation larger than ∼100 au and it is one of only three systems where both the L and T dwarfs are resolved at all—the others are Luhman 16AB (Luhman 2013) and SDSS J1416 +13AB (Burningham et al. 2010).

Assuming that W2150 is field age (see Section 7 above), we can find an analog to its mass ratio and binding energy among the young systems (<1 Gyr) compiled. For instance, the ∼2 Myr Chamaeleon star-forming region contains 2MASS J11011926-7732383AB (2M1101AB), an M7.25 and an M8.25 with a mass ratio of ∼0.5 and a separation of ∼240 au (Luhman 2004). As can be seen in Figures 8, 2M1101AB has a similar mass ratio and binding energy to W2150AB. At the time of its discovery, 2M1101AB was the first brown dwarf binary discovered with a separation >20 au and its existence was celebrated as a definitive insight into the formation of brown dwarfs. W2150AB now shows that such systems can survive into the field.

While it is intriguing to see the two systems with similar properties, they differ in age by several Gyr. Moreover, 2M1101AB is a member of Chamaeleon which is a densely crowded area of star formation compared to the sparsely separated field where we find W2150AB. While we have no idea how or where W2150AB formed, we can investigate the feasibility that it could have formed like 2M1101AB and survived dynamical interactions in its natal cluster and the Galaxy until a field age. As was discussed in Burgasser et al. (2003) and adapted in Close et al. (2007), systems with total

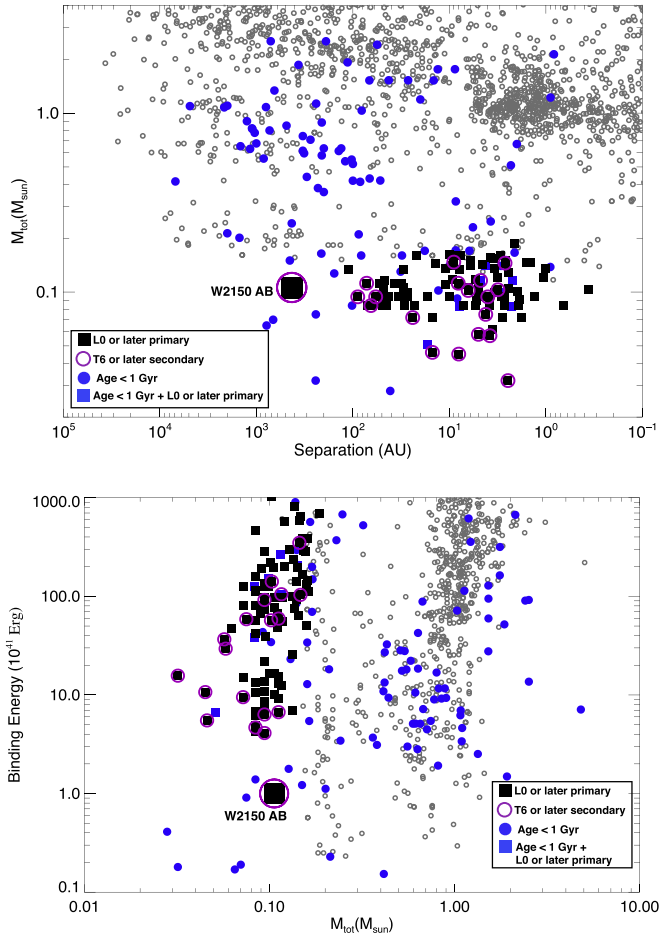

Figure 7. Collection of systems from the literature representing co-moving or binary companions. Systems with ages <1 Gyr are plotted as blue and field age objects are either light gray or black. If the system contains at least an L dwarf or later primary, we plotted the system as a black square. If it also contained a T6 or later secondary we plotted the system with an open purple circle. We show total mass vs. separation on the top panel and total mass vs. binding energy on the lower panel. W2150AB stands out as the lowest binding energy system not in a young cluster.

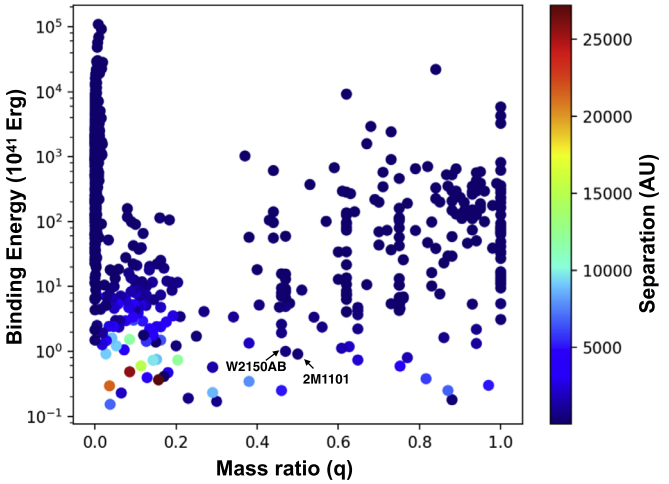

Figure 8. Same systems plotted as in Figure 7. In this case we show the mass ratio (q) vs. binding energy and color code the systems by their physical separation.

masses $\sim 0.1\,M_{\odot}$ will be stable against any type of stellar encounter as long as the separation is <1800 au and the number density of stellar perturbers is on the order of the measured Galactic disk mass density (see Pham 1997; Holmberg & Flynn 2000). W2150AB meets these criteria. Consequently, it is not altogether surprising that W2150AB exists—even though no other system had been discovered to date that rivals its properties in the field. What is surprising, and has been discussed at length concerning the difference between young systems discovered and those in the field, is whether very low-mass companions born in star-forming regions should become unstable and evaporate over time given their more dense natal environments. Burgasser et al. (2003) postulated how the local stellar density at birth impacts the viability of a pair surviving. Close et al. (2007) built upon that work and examined the stellar density for clusters such as Chamaeleon, Rho Ophiucus, Upper Scorpius, etc., where the bulk of the young sources from Figure 7 have been discovered. Consequently, Close et al. suggested that the majority of young systems (including 2M1101AB) were in the process of evaporating. Following this logic, W2150AB could either be considered a system that formed in a low-density environment (small sparse cluster for instance) or it was perturbed into its wide configuration while in a more dense cluster but the environment dispersed before it could evaporate the binary, leaving the system stable in the less dense field environment.

Another possible explanation for the survival of this source to field age could be that one of its components is in reality a closely separated binary system, making this a hierarchical triple system while increasing the overall binding energy. To test the latter hypothesis, we followed the prescription of Burgasser et al. (2010) to identify spectral binary systems from near-infrared, low-resolution, SpeX spectra. However, we do not find peculiarities in the spectrum of the primary attributable to unresolved binarity. Unfortunately this technique is not applicable for T8 objects, therefore we cannot rule out that the secondary might harbor an unseen companion.

Regardless of the reason it has survived until today, the total estimated mass of the system is $0.106\,M_{\rm Sun}$. So with a physical separation as large as 341 au, the binding energy ($E_{\rm bin} = 10^{41}$ erg) of W2150AB is the lowest found among ultracool dwarf objects not identified in a young cluster.

10. Discussion

We report the discovery of a resolved L1+T8 co-moving system: W2150AB with a physical separation of ~341 au. This discovery was enabled by a dedicated cohort of citizen scientists participating in the Backyard Worlds: Planet 9 citizen science project. The cool secondary appeared in no online catalogs, so it had eluded astronomers performing automated searches.

We obtained Magellan FIRE prism near-infrared spectra for both the primary and secondary and found both sources appear comparable to field sources with no deviant or peculiar features. The primary in the system is also a *Gaia*-detected source and has a well determined parallax of 41.3593 ± 0.2799 mas and proper motion components of $(\mu_{\rm ra}\cos({\rm decl.}), \mu_{\rm decl.}) = (888.627 \pm 0.502, -298.234 \pm 0.518)$ mas. Assuming an age range for the system of 0.5–10 Gyr we find that W2150A has $\log(L_{\rm bol}/L_{\odot}) = -3.69 \pm 0.01$, $T_{\rm eff} = 2118 \pm 62$ K, $\log g = 5.2 \pm 0, 2$, radius $= 1.03 \pm 0.06 R_{\rm Jup}$ and an estimated mass $= 72 \pm 12\ M_{\rm Jup}$ while W2150B has $\log(L_{\rm bol}/L_{\odot}) = -5.64 \pm 0.02$, $T_{\rm eff} = 719 \pm 61$ K, $\log g = 4.9 \pm 0, 5$, radius $= 0.95 \pm 0.16\,R_{\rm Jup}$ and an estimated mass $= 34 \pm 22\ M_{\rm Jup}$. The total estimated mass of the system is

Table 2
Companion Systems with Total Mass $< 0.2\,M_{\rm Sun}$

Name[a]	R.A.[b]	Decl.[b]	SpT_{M1}	SpT_{M2}	$Mass_{M1}$[c] ($M_{\rm Sun}$)	$Mass_{M2}$[c] ($M_{\rm Sun}$)	$M_{\rm tot}$ ($M_{\rm Sun}$)	(q)	Sep (au)	$E_{\rm bin}$[d] ($\times 10^{41}$ erg)	Young?[e]	Reference
(1)	(2)	(3)	(4)	(5)	(6)	(7)	(8)	(9)	(10)	(11)	(12)	(13)
FUTau	04 23 35.38	+25 03 03.0	M7.25	M9.25	0.05	0.015	0.065	0.30	784	0.17	Yng	68
Oph-11	16 22 25.20	−24 05 14.0	M9	M9.5	0.017	0.015	0.032	0.88	243	0.18	Yng	49
UScoCTIO-108	16 05 53.94	−18 18 42.7	M7	M9.5	0.057	0.013	0.07	0.23	670	0.19	Yng	10
1258+4013	12 58 35.01	+40 13 08.3	M6	M7	0.105	0.091	0.196	0.87	6700	0.25	Not Yng	79
NLTT730	00 15 02.40	+29 59 29.8	M4	L7.5	0.125	0.058	0.183	0.46	5070	0.25	Not Yng	37
0126-5022	01 26 55.50	−50 22 39.0	M6.5	M8	0.095	0.092	0.187	0.97	5100	0.30	Not Yng	3
2M1207	12 07 33.40	−39 32 54.0	M8	L5	0.024	0.004	0.028	0.17	41	0.41	Yng	29
LHS6176	09 50 47.28	+01 17 34.3	M4	T8	0.125	0.036	0.161	0.29	1400	0.57	Not Yng	69
LHS2803	13 48 02.90	−13 44 07.1	M4.5	T5	0.125	0.036	0.161	0.29	1400	0.57	Not Yng	36
Koenigstuhl-1	00 21 05.91	−42 44 43.5	M6	M9.5	0.103	0.079	0.182	0.77	1800	0.80	Not Yng	28
1101-7732	11 01 19.26	−77 32 38.3	M7	M8	0.05	0.025	0.075	0.50	242	0.91	Yng	67
2150-7520	21 50 18.99	−75 20 54.6	L1	T8	0.072	0.034	0.106	0.47	430	1.00	Not Yng	96
LP261-75	09 51 05.49	+35 58 02.1	M4.5	L6	0.125	0.025	0.15	0.20	450	1.22	Yng	83
1328+0808	13 28 35.49	+08 08 19.5	M6	M8.5	0.1	0.094	0.194	0.94	1250	1.32	Not Yng	97
VHS1256	12 56 01.92	−12 57 23.9	M7.5	L7	0.073	0.011	0.084	0.15	102	1.39	Yng	42
LP417	00 06 49.16	−08 52 46.3	M8.5	M9	0.094	0.081	0.175	0.86	820	1.63	Not Yng	24
Wolf940B	21 46 38.82	−00 10 38.6	M4	T8.5	0.125	0.031	0.156	0.25	400	1.71	Not Yng	26
0219-3925	02 19 22.10	−39 25 22.5	M6	L4	0.113	0.014	0.127	0.12	156	1.78	Yng	5
NLTT26746	11 15 01.22	+16 07 00.8	M4	L4	0.125	0.058	0.183	0.46	661	1.93	Not Yng	37
1631+2948	16 31 26.17	+29 48 47.1	M5.5	M8	0.1	0.094	0.194	0.94	756	2.19	Not Yng	97
1118-0640	11 18 06.99	−06 40 07.8	M4.5	T2	0.125	0.07	0.195	0.56	650	2.37	Not Yng	87
NLTT31450	12 39 49.19	+32 09 03.1	M4	L6	0.125	0.058	0.183	0.46	487	2.62	Not Yng	37
2233+0022	22 33 48.82	+00 22 14.0	L5	T4	0.058	0.036	0.094	0.62	90	4.08	Not Yng	71
1416+1348	14 16 23.94	+13 48 36.3	L7	T7.5	0.058	0.036	0.094	0.62	89	4.11	Not Yng	27
0205+1421	02 05 29.62	+14 21 14.0	T1	T3	0.048	0.036	0.084	0.75	71	4.28	Not Yng	35
0047+1546	00 47 57.41	+15 46 41.4	L8	T7	0.048	0.036	0.084	0.75	65	4.68	Not Yng	35
2229+0102	22 29 58.30	+01 02 17.2	T1	T5	0.048	0.036	0.084	0.75	62	4.91	Not Yng	35
0551-4434	05 51 46.00	−44 34 12.2	M8.5	L0	0.085	0.079	0.164	0.93	220	5.37	Not Yng	12
Oph-16	16 23 36.09	−24 02 20.9	M5	M5.5	0.095	0.069	0.164	0.73	212	5.44	Yng	33
1711+3500	17 11 04.60	+35 00 36.8	T8	T9.5	0.031	0.015	0.046	0.48	15	5.52	Not Yng	65

Notes.
[a] The name used is a shorthand from the discovery paper or from the coordinates of the primary.
[b] The R.A. and decl. listed are of the primary in the system.
[c] Masses were either obtained from dynamical mass measurements (and noted as such), discovery paper estimates or by applying the spectral type to mass relation from Dupuy & Liu (2017).
[d] To account for a distribution of the eccentricities of the binary orbits, we multiply the physical separation by 1.26 and use this value to compute the binding energy.
[e] Yng indicates a source is associated with a cluster/moving-group/star-forming region with an age <1 Gyr. Not Yng indicates no associated region therefore a field age for the source.
[f] Dynamical masses from Dupuy & Liu (2017).
[g] Total masses were listed in Dupuy & Liu (2017) but individual masses were not therefore we used the relation in that work to estimate object masses.
[h] Dynamical masses from Garcia et al. (2017).

References. 1 = Allers et al. (2009), 2 = Allers et al. (2010), 3 = Artigau et al. (2007), 4 = Artigau et al. (2011), 5 = Artigau et al. (2015), 6 = Bardalez Gagliuffi et al. (2014), 7 = Bardalez Gagliuffi et al. (2015), 8 = Basri & Martín (1999), 9 = Batista et al. (2011), 10 = Béjar et al. (2008), 11 = Biller et al. (2006), 12 = Billères et al. (2005), 13 = Bouy et al. (2003), 14 = Bouy et al. (2004), 15 = Burgasser et al. (2003), 16 = Burgasser et al. (2004), 17 = Burgasser et al. (2005), 18 = Burgasser et al. (2006), 19 = Burgasser & McElwain (2006), 20 = Burgasser (2007), 21 = Burgasser et al. (2008), 22 = Burgasser et al. (2009), 23 = Burgasser et al. (2010), 24 = Burgasser et al. (2012), 25 = Burgasser et al. (2015), 26 = Burningham et al. (2009), 27 = Burningham et al. (2010), 28 = Caballero (2007), 29 = Chauvin et al. (2004), 30 = Close et al. (2002a), 31 = Close et al. (2002b), 32 = Close et al. (2003), 33 = Close et al. (2007), 34 = Dahn et al. (2008), 35 = Day-Jones et al. (2013), 36 = Deacon et al. (2012), 37 = Deacon et al. (2014), 38 = Delfosse et al. (1997), 39 = Dhital et al. (2011), 40 = Forveille et al. (2005), 41 = Freed et al. (2003), 42 = Gauza et al. (2015), 43 = Geißler et al. (2011), 44 = Gelino & Burgasser (2010), 45 = Gelino et al. (2011), 46 = Gizis et al. (2003), 47 = Golimowski et al. (2004), 48 = Guenther & Wuchterl (2003), 49 = Jayawardhana & Ivanov (2006), 50 = Kellogg et al. (2015), 51 = Kendall et al. (2007), 52 = Kenworthy et al. (2001), 53 = Kirkpatrick et al. (2001), 54 = Kirkpatrick et al. (2010), 55 = Kirkpatrick et al. (2011), 56 = Koerner et al. (1999), 57 = Konopacky et al. (2007), 58 = Kraus et al. (2005), 59 = Kraus et al. (2006), 60 = Law et al. (2006), 61 = Leinert et al. (2000), 62 = Liu et al. (2006), 63 = Liu et al. (2010), 64 = Liu et al. (2011), 65 = Liu et al. (2012), 66 = Looper et al. (2008), 67 = Luhman (2004), 68 = Luhman et al. (2009), 69 = Luhman et al. (2012), 70 = Luhman (2013), 71 = Marocco et al. (2015), 72 = Martín (2003), 73 = Martín et al. (1998), 74 = McCaughrean et al. (2004), 75 = Montagnier et al. (2006), 76 = Mugrauer et al. (2007), 77 = Potter et al. (2002), 78 = Radigan et al. (2008), 79 = Radigan et al. (2009), 80 = Radigan et al. (2013), 81 = Reid et al. (2001), 82 = Reid et al. (2002), 83 = Reid & Walkowicz (2006), 84 = Reid et al. (2006a), 85 = Reid et al. (2006b), 86 = Reid et al. (2008), 87 = Reylé et al. (2014), 88 = Sahlmann et al. (2013), 89 = Seifahrt et al. (2005), 90 = Siegler et al. (2003), 91 = Siegler et al. (2005), 92 = Siegler et al. (2007), 93 = Stassun et al. (2006), 94 = Stumpf et al. (2008), 95 = Stumpf et al. (2010), 96 = this paper, 97 = Zhang et al. (2010), 98 = Dupuy & Liu (2017).
(This table is available in its entirety in machine-readable form.)

Table 3
Companion Systems with Total Mass $< 0.2\ M_{\rm Sun}^{\rm d}$

Name	R.A. Prim	Decl. Prim	π Prim (mas)	μ_α Prim (mas yr^{-1})	μ_δ Prim (mas yr^{-1})	G Prim	R.A. Sec	Decl. Sec	π Sec (mas)	μ_α Sec (mas yr^{-1})	μ_δ Sec (mas yr^{-1})	G Sec
(1)	(2)	(3)	(4)	(5)	(6)	(7)	(8)	(9)	(10)	(11)	(12)	(13)
FUTau	04 23 35.39	+25 03 02.7	7.5981 ± 0.1497	6.895 ± 0.376	−21.026 ± 0.202	15.24	04 23 35.73	+25 02 59.6	7.4909 ± 1.2887	12.450 ± 4.056	−21.761 ± 1.903	20.48
Oph-11	16 22 25.20	−24 05 13.6	7.3440 ± 0.4060	−15.790 ± 0.698	−23.236 ± 0.520	18.92	16 22 25.19	−24 05 15.9	…	…	…	20.24
UScoCTIO-108	16 05 54.07	−18 18 44.3	6.9306 ± 0.2409	−10.156 ± 0.454	−20.618 ± 0.260	17.42	…	…	…	…	…	…
1258+4013	12 58 35.01	+40 13 08.1	8.4520 ± 0.3382	79.289 ± 0.356	−111.430 ± 0.445	19.17	12 58 37.99	+40 14 01.5	7.3800 ± 0.5788	77.913 ± 0.539	−109.434 ± 0.833	19.83
NLTT730	00 15 05.73	+29 55 40.3	28.6060 ± 0.0709	381.542 ± 0.103	−227.076 ± 0.077	14.11	…	…	…	…	…	…
0126-5022	01 26 55.50	−50 22 38.7	13.9950 ± 0.2440	140.207 ± 0.333	−50.356 ± 0.311	18.80	01 27 02.83	−50 23 20.9	14.4188 ± 0.3546	146.684 ± 0.442	−45.784 ± 0.421	19.28
2M1207	12 07 33.46	−39 32 54.0	15.5242 ± 0.1561	−64.083 ± 0.233	−23.720 ± 0.130	17.41	…	…	…	…	…	…
LHS6176	09 50 49.59	+01 18 13.6	50.8011 ± 0.0762	234.644 ± 0.109	−360.553 ± 0.096	12.63	…	…	…	…	…	…
LHS2803	13 48 07.27	−13 44 31.5	54.9974 ± 0.0838	−687.597 ± 0.144	−512.979 ± 0.124	13.54	…	…	…	…	…	…
Koenigstuhl-1	00 21 10.74	−42 45 40.1	37.3985 ± 0.0727	255.046 ± 0.088	−12.530 ± 0.092	15.37	00 21 05.91	−42 44 43.4	38.5223 ± 0.5439	258.636 ± 0.733	−1.884 ± 0.702	18.35
1101-7732	11 01 19.19	−77 32 38.7	5.4081 ± 0.1877	−22.653 ± 0.435	2.062 ± 0.397	18.33	11 01 19.42	−77 32 37.5	5.4333 ± 0.3368	−23.668 ± 0.748	1.931 ± 0.723	19.40
W2150	21 50 15.77	−75 20 36.7	41.3593 ± 0.2799	888.627 ± 0.502	−298.234 ± 0.518	18.91	…	…	…	…	…	…
LP261-75	09 51 04.44	35 58 06.7	29.4464 ± 0.1376	−100.975 ± 0.142	−171.822 ± 0.126	13.83	…	…	…	…	…	…
1328+0808	13 28 35.39	08 08 18.8	9.2012 ± 0.3601	−148.679 ± 0.718	−57.100 ± 0.418	19.07	…	…	…	…	…	…
VHS1256	12 56 01.84	−12 57 24.8	…	…	…	15.05	…	…	…	…	…	…
LP417	00 06 47.39	−08 52 40.3	31.9418 ± 0.1585	−61.010 ± 0.328	−321.353 ± 0.181	15.66	00 06 49.09	−08 52 51.13	34.0726 ± 0.3914	−57.330 ± 0.724	−321.090 ± 0.395	18.71
Wolf940B	21 46 41.22	−00 10 31.6	80.7724 ± 0.1102	769.495 ± 0.120	−505.666 ± 0.123	11.31	…	…	…	…	…	…
0219-3925	02 19 22.24	−39 25 23.0	24.9441 ± 0.1207	103.614 ± 0.138	−35.865 ± 0.143	15.01	…	…	…	…	…	…
NLTT26746	11 15 01.05	16 06 42.3	24.5836 ± 0.0488	−252.512 ± 0.102	−144.731 ± 0.083	13.99	…	…	…	…	…	…
1631+2948	16 31 26.13	29 48 47.1	10.3661 ± 0.1382	−42.416 ± 0.212	−0.240 ± 0.241	17.81	16 31 26.12	29 48 36.83	10.5547 ± 0.4138	−41.831 ± 0.592	−3.693 ± 0.680	19.63
1118-0640	11 18 06.79	−06 40 08.4	9.9041 ± 0.1540	−200.255 ± 0.289	−48.180 ± 0.185	17.21	…	…	…	…	…	…
NLTT31450	12 39 49.32	32 08 50.0	25.8908 ± 0.0514	−24.553 ± 0.077	−193.677 ± 0.053	13.64	…	…	…	…	…	…
2233+0022	…	…	…	…	…	…	…	…	…	…	…	…
1416+1348	14 16 24.16	13 48 28.1	107.5599 ± 0.2958	85.692 ± 0.694	129.071 ± 0.465	18.33	…	…	…	…	…	…
0205+1421	…	…	…	…	…	…	…	…	…	…	…	…
0047+1546	…	…	…	…	…	…	…	…	…	…	…	…
2229+0102	…	…	…	…	…	…	…	…	…	…	…	…
0551-4434	05 51 45.94	−44 34 13.4	9.0080 ± 0.7829	−60.535 ± 1.536	−13.364 ± 1.775	20.57	05 51 45.94	−44 34 11.28	7.1950 ± 1.5168	−62.484 ± 3.394	−16.180 ± 3.207	20.91
Oph-16	16 23 36.11	−24 02 21.2	6.7247 ± 0.1411	−6.136 ± 0.299	−26.436 ± 0.188	15.97	16 23 36.03	−24 02 22.56	7.0935 ± 0.1463	−8.859 ± 0.277	−26.194 ± 0.174	16.45
1711+3500	…	…	…	…	…	…	…	…	…	…	…	…

(This table is available in its entirety in machine-readable form.)

0.106 M_{Sun} hence with a physical separation as large as 341 au, the binding energy ($E_{bin} = 10^{41}$ erg) is the lowest found among ultracool dwarf objects not identified in a young cluster. In separation, E_{bin}, and mass ratio, W2150AB resembles 2M1101AB, the first brown dwarf binary discovered with a separation >20 au. 2M1101AB, discovered in the Chamaeleon star-forming region, was heralded as a source of definitive insight into the formation of brown dwarfs. But W2150AB leaves us with an intriguing question about whether it is an evolved version of 2M1101AB or perhaps a system that formed in a low-density cluster that survived unperturbed by interactions with nearby stellar or giant molecular clouds. Given that it is easily resolved with ground- or space-based observatories, W2150AB is an excellent benchmark system for understanding how brown dwarfs form and evolve together.

The Backyard Worlds: Planet 9 team would like to thank the many Zooniverse volunteers who have participated in this project, from providing feedback during the beta review stage to classifying flipbooks to contributing to the discussions on TALK. We would also like to thank the Zooniverse web development team for their work creating and maintaining the Zooniverse platform and the Project Builder tools. This research was supported by NASA Astrophysics Data Analysis Program grant NNH17AE75I.

This research has made use of: the Washington Double Star Catalog maintained at the U.S. Naval Observatory; the SIMBAD database and VizieR catalog access tool, operated at the Centre de Donnees astronomiques de Strasbourg, France (Ochsenbein et al. 2000); data products from the Two Micron All Sky Survey (2MASS; Skrutskie et al. 2006), which is a joint project of the University of Massachusetts and the Infrared Processing and Analysis Center (IPAC)/California Institute of Technology (Caltech), funded by the National Aeronautics and Space Administration (NASA) and the National Science Foundation; data products from the *Wide-field Infrared Survey Explorer* (*WISE*; and Wright et al. 2010), which is a joint project of the University of California, Los Angeles, and the Jet Propulsion Laboratory (JPL)/Caltech, funded by NASA. This project was developed in part at the 2017 Heidelberg *Gaia* Sprint, hosted by the Max-Planck-Institut fur Astronomie, Heidelberg. A.M.M. acknowledges support from Hubble Fellowship HST-HF2-51415.001-A and NASA ADAP grant NNH17AE75I. S.E.L. is supported by an appointment to the NASA Postdoctoral Program at NASA Goddard Space Flight Center, administered by Universities Space Research Association under contract with NASA. This work has made use of data from the European Space Agency (ESA) mission *Gaia*, processed by the *Gaia* Data Processing and Analysis Consortium. Funding for the DPAC has been provided by national institutions, in particular the institutions participating in the *Gaia* Multilateral Agreement.

Facilities: *Gaia*, Hale(TripleSpec), *WISE*, CTIO:2MASS, *UKIRT*.

Software: Aladin, BANYAN Σ (Gagné et al. 2018).

ORCID iDs

Jacqueline K. Faherty https://orcid.org/0000-0001-6251-0573
Sam Goodman https://orcid.org/0000-0003-2236-2320
Dan Caselden https://orcid.org/0000-0001-7896-5791
Guillaume Colin https://orcid.org/0000-0002-7630-1243
Marc J. Kuchner https://orcid.org/0000-0002-2387-5489
Aaron M. Meisner https://orcid.org/0000-0002-1125-7384
Jonathan Gagné https://orcid.org/0000-0002-2592-9612
Adam C. Schneider https://orcid.org/0000-0002-6294-5937
Eileen C. Gonzales https://orcid.org/0000-0003-4636-6676
Daniella C. Bardalez Gagliuffi https://orcid.org/0000-0001-8170-7072
Sarah E. Logsdon https://orcid.org/0000-0002-9632-9382
Katelyn Allers https://orcid.org/0000-0003-0580-7244
Adam J. Burgasser https://orcid.org/0000-0002-6523-9536

References

Allers, K. N., & Liu, M. C. 2013, ApJ, 772, 79
Allers, K. N., Liu, M. C., Dupuy, T. J., & Cushing, M. C. 2010, ApJ, 715, 561
Allers, K. N., Liu, M. C., Shkolnik, E., et al. 2009, ApJ, 697, 824
Artigau, É., Gagné, J., Faherty, J., et al. 2015, ApJ, 806, 254
Artigau, É., Lafrenière, D., Albert, L., & Doyon, R. 2009, ApJ, 692, 149
Artigau, É., Lafrenière, D., Doyon, R., et al. 2007, ApJL, 659, L49
Artigau, É., Lafrenière, D., Doyon, R., et al. 2011, ApJ, 739, 48
Bardalez Gagliuffi, D. C., Burgasser, A. J., Gelino, C. R., et al. 2014, ApJ, 794, 143
Bardalez Gagliuffi, D. C., Gelino, C. R., & Burgasser, A. J. 2015, AJ, 150, 163
Barnes, S. A. 2007, ApJ, 669, 1167
Basri, G., & Martín, E. L. 1999, AJ, 118, 2460
Bate, M. R. 2011, MNRAS, 417, 2036
Bate, M. R., Bonnell, I. A., & Bromm, V. 2002, MNRAS, 332, L65
Batista, V., Gould, A., Dieters, S., et al. 2011, A&A, 529, A102
Béjar, V. J. S., Zapatero Osorio, M. R., Pérez-Garrido, A., et al. 2008, ApJL, 673, L185
Biller, B. A., Kasper, M., Close, L. M., Brandner, W., & Kellner, S. 2006, ApJL, 641, L141
Billères, M., Delfosse, X., Beuzit, J.-L., et al. 2005, A&A, 440, L55
Bochanski, J. J., Hennawi, J. F., Simcoe, R. A., et al. 2009, PASP, 121, 1409
Bouy, H., Brandner, W., Martín, E. L., et al. 2003, AJ, 126, 1526
Bouy, H., Brandner, W., Martín, E. L., et al. 2004, A&A, 424, 213
Burgasser, A. J. 2007, AJ, 134, 1330
Burgasser, A. J., Cruz, K. L., Cushing, M., et al. 2010, ApJ, 710, 1142
Burgasser, A. J., Dhital, S., & West, A. A. 2009, AJ, 138, 1563
Burgasser, A. J., Gillon, M., Melis, C., et al. 2015, AJ, 149, 104
Burgasser, A. J., Kirkpatrick, J. D., Cruz, K. L., et al. 2006, ApJS, 166, 585
Burgasser, A. J., Kirkpatrick, J. D., & Lowrance, P. J. 2005, AJ, 129, 2849
Burgasser, A. J., Kirkpatrick, J. D., Reid, I. N., et al. 2003, ApJ, 586, 512
Burgasser, A. J., Liu, M. C., Ireland, M. J., Cruz, K. L., & Dupuy, T. J. 2008, ApJ, 681, 579
Burgasser, A. J., Luk, C., Dhital, S., et al. 2012, ApJ, 757, 110
Burgasser, A. J., & McElwain, M. W. 2006, AJ, 131, 1007
Burgasser, A. J., McElwain, M. W., Kirkpatrick, J. D., et al. 2004, AJ, 127, 2856
Burningham, B., Cardoso, C. V., Smith, L., et al. 2013, MNRAS, 433, 457
Burningham, B., Leggett, S. K., Lucas, P. W., et al. 2010, MNRAS, 404, 1952
Burningham, B., Pinfield, D. J., Leggett, S. K., et al. 2009, MNRAS, 395, 1237
Caballero, J. A. 2007, ApJ, 667, 520
Caselden, D., Westin, P., III, Meisner, A., Kuchner, M., & Colin, G. 2018, WiseView: Visualizing motion and variability of faint WISE sources, Astrophysics Source Code Library, ascl:1806.004
Casewell, S. L., Jameson, R. F., & Burleigh, M. R. 2008, MNRAS, 390, 1517
Chauvin, G., Lagrange, A.-M., Dumas, C., et al. 2004, A&A, 425, L29
Close, L. M., Potter, D., Brandner, W., et al. 2002a, ApJ, 566, 1095
Close, L. M., Siegler, N., Freed, M., & Biller, B. 2003, ApJ, 587, 407
Close, L. M., Siegler, N., Potter, D., Brand ner, W., & Liebert, J. 2002b, ApJL, 567, L53
Close, L. M., Zuckerman, B., Song, I., et al. 2007, ApJ, 660, 1492
Cruz, K. L., Kirkpatrick, J. D., & Burgasser, A. J. 2009, AJ, 137, 3345
Cushing, M. C., Kirkpatrick, J. D., Gelino, C. R., et al. 2011, ApJ, 743, 50
Cushing, M. C., Looper, D., Burgasser, A. J., et al. 2009, ApJ, 696, 986
Cushing, M. C., Vacca, W. D., & Rayner, J. T. 2004, PASP, 116, 362
Cutri, R. M., Skrutskie, M. F., van Dyk, S., et al. 2003, yCat, 2246, 0
Dahn, C. C., Harris, H. C., Levine, S. E., et al. 2008, ApJ, 686, 548
Day-Jones, A. C., Marocco, F., Pinfield, D. J., et al. 2013, MNRAS, 430, 1171
Deacon, N. R., Hambly, N. C., & Cooke, J. A. 2005, A&A, 435, 363
Deacon, N. R., Liu, M. C., Magnier, E. A., et al. 2012, ApJ, 757, 100
Deacon, N. R., Liu, M. C., Magnier, E. A., et al. 2014, ApJ, 792, 119
Debes, J. H., Thévenot, M., Kuchner, M. J., et al. 2019, ApJL, 872, L25
Delfosse, X., Tinney, C. G., Forveille, T., et al. 1997, A&A, 327, L25

DENIS Consortium 2005, yCat, 2263, 0
Dhital, S., Burgasser, A. J., Looper, D. L., & Stassun, K. G. 2011, AJ, 141, 7
Dieterich, S. B., Weinberger, A. J., Boss, A. P., et al. 2018, ApJ, 865, 28
Dupuy, T. J., & Kraus, A. L. 2013, Sci, 341, 1492
Dupuy, T. J., & Liu, M. C. 2012, ApJS, 201, 19
Dupuy, T. J., & Liu, M. C. 2017, ApJS, 231, 15
Faherty, J. K., Burgasser, A. J., Bochanski, J. J., et al. 2011, AJ, 141, 71
Faherty, J. K., Burgasser, A. J., Cruz, K. L., et al. 2009, AJ, 137, 1
Faherty, J. K., Burgasser, A. J., Walter, F. M., et al. 2012, ApJ, 752, 56
Faherty, J. K., Burgasser, A. J., West, A. A., et al. 2010, AJ, 139, 176
Faherty, J. K., Rice, E. L., Cruz, K. L., Mamajek, E. E., & Núñez, A. 2013, AJ, 145, 2
Faherty, J. K., Riedel, A. R., Cruz, K. L., et al. 2016, ApJS, 225, 10
Filippazzo, J. C., Rice, E. L., Faherty, J., et al. 2015, ApJ, 810, 158
Forveille, T., Beuzit, J.-L., Delorme, P., et al. 2005, A&A, 435, L5
Freed, M., Close, L. M., & Siegler, N. 2003, ApJ, 584, 453
Gagné, J., Faherty, J. K., Burgasser, A. J., et al. 2017, ApJL, 841, L1
Gagné, J., Mamajek, E. E., Malo, L., et al. 2018, ApJ, 856, 23
Gaia Collaboration, Prusti, T., de Bruijne, J. H. J., et al. 2016, A&A, 595, A1
Garcia, E. V., Ammons, S. M., Salama, M., et al. 2017, ApJ, 846, 97
Gauza, B., Béjar, V. J. S., Pérez-Garrido, A., et al. 2015, ApJ, 804, 96
Geißler, K., Metchev, S., Kirkpatrick, J. D., Berriman, G. B., & Looper, D. 2011, ApJ, 732, 56
Gelino, C. R., & Burgasser, A. J. 2010, AJ, 140, 110
Gelino, C. R., Kirkpatrick, J. D., Cushing, M. C., et al. 2011, AJ, 142, 57
Gillon, M., Triaud, A. H. M. J., Demory, B.-O., et al. 2017, Natur, 542, 456
Gizis, J. E., Reid, I. N., Knapp, G. R., et al. 2003, AJ, 125, 3302
Golimowski, D. A., Henry, T. J., Krist, J. E., et al. 2004, AJ, 128, 1733
Gonzales, E. C., Faherty, J. K., Gagné, J., Artigau, É., & Bardalez Gagliuffi, D. 2018, ApJ, 864, 100
Goodwin, S. P., & Whitworth, A. 2007, A&A, 466, 943
Guenther, E. W., & Wuchterl, G. 2003, A&A, 401, 677
Holmberg, J., & Flynn, C. 2000, MNRAS, 313, 209
Jayawardhana, R., & Ivanov, V. D. 2006, Sci, 313, 1279
Kellogg, K., Metchev, S., Geißler, K., et al. 2015, AJ, 150, 182
Kendall, T. R., Jones, H. R. A., Pinfield, D. J., et al. 2007, MNRAS, 374, 445
Kenworthy, M., Hofmann, K.-H., Close, L., et al. 2001, ApJL, 554, L67
Kirkpatrick, J. D., Cushing, M. C., Gelino, C. R., et al. 2011, ApJS, 197, 19
Kirkpatrick, J. D., Dahn, C. C., Monet, D. G., et al. 2001, AJ, 121, 3235
Kirkpatrick, J. D., Kellogg, K., Schneider, A. C., et al. 2016, ApJS, 224, 36
Kirkpatrick, J. D., Looper, D. L., Burgasser, A. J., et al. 2010, ApJS, 190, 100
Kirkpatrick, J. D., Martin, E. C., Smart, R. L., et al. 2019, ApJS, 240, 19
Kirkpatrick, J. D., Reid, I. N., Liebert, J., et al. 1999, ApJ, 519, 802
Kirkpatrick, J. D., Schneider, A., Fajardo-Acosta, S., et al. 2014, ApJ, 783, 122
Koerner, D. W., Kirkpatrick, J. D., McElwain, M. W., & Bonaventura, N. R. 1999, ApJL, 526, L25
Konopacky, Q. M., Ghez, A. M., Rice, E. L., & Duchêne, G. 2007, ApJ, 663, 394
Kraus, A. L., White, R. J., & Hillenbrand, L. A. 2005, ApJ, 633, 452
Kraus, A. L., White, R. J., & Hillenbrand, L. A. 2006, ApJ, 649, 306
Kuchner, M. J., Faherty, J. K., Schneider, A. C., et al. 2017, ApJL, 841, L19
Lagrange, A.-M., Bonnefoy, M., Chauvin, G., et al. 2010, Sci, 329, 57
Lang, D. 2014, AJ, 147, 108
Law, N. M., Hodgkin, S. T., & Mackay, C. D. 2006, MNRAS, 368, 1917
Leggett, S. K., Burningham, B., Saumon, D., et al. 2010, ApJ, 710, 1627
Leggett, S. K., Tremblin, P., Esplin, T. L., Luhman, K. L., & Morley, C. V. 2017, ApJ, 842, 118
Leinert, C., Allard, F., Richichi, A., & Hauschildt, P. H. 2000, A&A, 353, 691
Li, Y., Kouwenhoven, M. B. N., Stamatellos, D., & Goodwin, S. P. 2015, ApJ, 805, 116
Lindegren, L., Hernandez, J., Bombrun, A., et al. 2018, A&A, 616, A2
Liu, M. C., Delorme, P., Dupuy, T. J., et al. 2011, ApJ, 740, 108
Liu, M. C., Dupuy, T. J., & Allers, K. N. 2016, ApJ, 833, 96
Liu, M. C., Dupuy, T. J., Bowler, B. P., Leggett, S. K., & Best, W. M. J. 2012, ApJ, 758, 57
Liu, M. C., Dupuy, T. J., & Leggett, S. K. 2010, ApJ, 722, 311
Liu, M. C., Leggett, S. K., Golimowski, D. A., et al. 2006, ApJ, 647, 1393
Liu, M. C., Magnier, E. A., Deacon, N. R., et al. 2013, ApJL, 777, L20
Looper, D. L., Gelino, C. R., Burgasser, A. J., & Kirkpatrick, J. D. 2008, ApJ, 685, 1183
Luhman, K. L. 2004, ApJ, 614, 398
Luhman, K. L. 2013, ApJL, 767, L1
Luhman, K. L. 2014, ApJL, 786, L18
Luhman, K. L., Loutrel, N. P., McCurdy, N. S., et al. 2012, ApJ, 760, 152
Luhman, K. L., Mamajek, E. E., Allen, P. R., Muench, A. A., & Finkbeiner, D. P. 2009, ApJ, 691, 1265
Macintosh, B., Graham, J. R., Barman, T., et al. 2015, Sci, 350, 64
Mamajek, E. E., & Hillenbrand, L. A. 2008, ApJ, 687, 1264
Marocco, F., Jones, H. R. A., Day-Jones, A. C., et al. 2015, MNRAS, 449, 3651
Martín, E. L., Barrado y Navascués, D., Baraffe, I., Bouy, H., & Dahm, S. 2003, ApJ, 594, 525
Martín, E. L., Basri, G., Brandner, W., et al. 1998, ApJL, 509, L113
Martin, E. L., Brandner, W., & Basri, G. 1999, Sci, 283, 1718
McCaughrean, M. J., Close, L. M., Scholz, R.-D., et al. 2004, A&A, 413, 1029
Meisner, A. M., Lang, D., & Schlegel, D. J. 2017a, AJ, 154, 161
Meisner, A. M., Lang, D., & Schlegel, D. J. 2017b, AJ, 153, 38
Meisner, A. M., Lang, D., & Schlegel, D. J. 2018, AJ, 156, 69
Montagnier, G., Ségransan, D., Beuzit, J. L., et al. 2006, A&A, 460, L19
Morley, C. V., Skemer, A. J., Allers, K. N., et al. 2018, ApJ, 858, 97
Mugrauer, M., Seifahrt, A., & Neuhäuser, R. 2007, MNRAS, 378, 1328
Mužić, K., Radigan, J., Jayawardhana, R., et al. 2012, AJ, 144, 180
Naud, M.-E., Artigau, É., Malo, L., et al. 2014, ApJ, 787, 5
Ochsenbein, F., Bauer, P., & Marcout, J. 2000, A&AS, 143, 23
Padoan, P., & Nordlund, Å. 2004, ApJ, 617, 559
Pavlenko, Y. V., & Magazzu, A. 1996, A&A, 311, 961
Pham, H.-A. 1997, ESASP, 402, 559
Potter, D., Martín, E. L., Cushing, M. C., et al. 2002, ApJL, 567, L133
Radigan, J., Jayawardhana, R., Lafrenière, D., et al. 2013, ApJ, 778, 36
Radigan, J., Lafrenière, D., Jayawardhana, R., & Doyon, R. 2008, ApJ, 689, 471
Radigan, J., Lafrenière, D., Jayawardhana, R., & Doyon, R. 2009, ApJ, 698, 405
Reid, I. N., Cruz, K. L., Kirkpatrick, J. D., et al. 2008, AJ, 136, 1290
Reid, I. N., Gizis, J. E., Kirkpatrick, J. D., & Koerner, D. W. 2001, AJ, 121, 489
Reid, I. N., Kirkpatrick, J. D., Liebert, J., et al. 2002, AJ, 124, 519
Reid, I. N., Lewitus, E., Allen, P. R., Cruz, K. L., & Burgasser, A. J. 2006a, AJ, 132, 891
Reid, I. N., Lewitus, E., Burgasser, A. J., & Cruz, K. L. 2006b, ApJ, 639, 1114
Reid, I. N., & Walkowicz, L. M. 2006, PASP, 118, 671
Reipurth, B., & Clarke, C. 2001, AJ, 122, 432
Reylé, C., Delorme, P., Artigau, E., et al. 2014, A&A, 561, A66
Riedel, A. R., DiTomasso, V., Rice, E. L., et al. 2019, AJ, 157, 247
Sahlmann, J., Lazorenko, P. F., Ségransan, D., et al. 2013, A&A, 556, A133
Saumon, D., & Marley, M. S. 2008, ApJ, 689, 1327
Schlafly, E. F., Meisner, A. M., & Green, G. M. 2019, ApJS, 240, 30
Seifahrt, A., Mugrauer, M., Wiese, M., Neuhäuser, R., & Guenther, E. W. 2005, AN, 326, 974
Siegler, N., Close, L. M., Burgasser, A. J., et al. 2007, AJ, 133, 2320
Siegler, N., Close, L. M., Cruz, K. L., Martín, E. L., & Reid, I. N. 2005, ApJ, 621, 1023
Siegler, N., Close, L. M., Mamajek, E. E., & Freed, M. 2003, ApJ, 598, 1265
Simcoe, R. A., Burgasser, A. J., Schechter, P. L., et al. 2013, PASP, 125, 270
Skemer, A. J., Morley, C. V., Allers, K. N., et al. 2016, ApJL, 826, L17
Skrutskie, M. F., Cutri, R. M., Stiening, R., et al. 2006, AJ, 131, 1163
Stassun, K. G., Mathieu, R. D., & Valenti, J. A. 2006, Natur, 440, 311
Stumpf, M. B., Brandner, W., Bouy, H., Henning, T., & Hippler, S. 2010, A&A, 516, A37
Stumpf, M. B., Brandner, W., Henning, T., et al. 2008, arXiv:0811.0556
Tinney, C. G., Faherty, J. K., Kirkpatrick, J. D., et al. 2014, ApJ, 796, 39
Vacca, W. D., Cushing, M. C., & Rayner, J. T. 2003, PASP, 115, 389
Vrba, F. J., Henden, A. A., Luginbuhl, C. B., et al. 2004, AJ, 127, 2948
Wilson, J. C., Kirkpatrick, J. D., Gizis, J. E., et al. 2001, AJ, 122, 1989
Wright, E. L., Eisenhardt, P. R. M., Mainzer, A. K., et al. 2010, AJ, 140, 1868
Zhang, Z. H., Pinfield, D. J., Day-Jones, A. C., et al. 2010, MNRAS, 404, 1817